SLOPE STABILITY OF GEOSYNTHETIC CLAY LINER TEST PLOTS

In Cincinnati Ohio, fourteen large-scale test plots were constructed under the supervision of the US EPA to evaluate the slope stability of geosynthetic clay liners at low normal stresses when used in typical landfill cover applications. Five plots were constructed on slopes having a 3H:1V configuration and nine were constructed on slopes having a 2H:1V configuration. Plots were approximately 9 meters wide with the 2H:1V slopes 20 meters long and the 3H:1V slopes 29 meters long. Several different GCL configurations were evaluated in this study to determine the internal and interface shear parameters of the GCL's in their installed configurations.

All of the GCL-lined 3:1 slopes were found to be stable, with little or no internal or interface shear displacement occurring over several years of monitoring. Most of the 2:1 slopes were also stable, although sliding failures eventually occurred at the geomembrane-GCL interface as would be predicted by shear box testing.

Based on experience from these test plots, the practice of conducting laboratory direct shear tests on GCL's and using limit equilibrium methods to determine slope stability of design configurations has been validated. Analysis of these test plots has substantiated that current design methods can effectively predict the slope stability of a design.

800.527.9948 Fax 847.577.5566

SLOPE STABILITY OF GEOSYNTHETIC CLAY LINER TEST PLOTS

By David E. Daniel,[1] Robert M. Koerner,[2] Rudolph Bonaparte,[3] Robert E. Landreth,[4] David A. Carson,[5] and Heather B. Scranton[6]

ABSTRACT: Fourteen full-scale field test plots containing five types of geosynthetic clay liners (GCLs) were constructed on 2H:1V and 3H:1V slopes for the purpose of assessing slope stability. The test plots were designed to simulate typical final cover systems for landfills. Slides occurred in two of the 2H:1V test plots along interfaces between textured geomembranes and the woven geotextile components of internally reinforced GCLs. One additional slide occurred within the unreinforced GCL component of a 2H:1V test plot, when the GCL unexpectedly became hydrated. All 3H:1V slopes have remained stable. Results of laboratory direct shear tests compared favorably with field observations, providing support for the current design procedures that engineers are using for assessing the stability of slopes containing GCLs.

INTRODUCTION

Geosynthetic clay liners (GCLs), which consist of a thin layer of bentonite sandwiched between two geotextiles or mixed with an adhesive and attached to a geomembrane, are a relatively new type of linear material receiving widespread use in landfill liner and final cover systems. Information on GCLs may be found in Koerner (1994), Daniel and Koerner (1995), Koerner and Gartung (1995), Well (1997), and the references therein.

While GCLs enjoy many favorable hydraulic characteristics, they suffer from limitations as a result of the low shear strength of hydrated bentonite (Mesri and Olson 1970; Olson 1974; and Gilbert et al. 1996). A shearing failure involving a GCL can occur at three possible locations: (1) The external interface between the top of the GCL and the overlying material (soil or geosynthetic); (2) internally within the GCL; and (3) the external interface between the bottom of the GCL and the underlying material (soil or geosynthetic). Current engineering design practice is to establish appropriate internal and interface shear strength parameters for design using direct shear tests on 300-mm^2 test specimens and employing traditional limit equilibrium techniques for analyzing slope stability. However, the low shear strength of bentonite, the limited number of laboratory test results available, the inherent limitations of laboratory direct shear tests, the uncertainty over use of peak versus residual shear strength, the newness of GCLs, and the lack of field experience with GCLs all lead to questions about the long-term stability of GCLs on relatively steep slopes.

The project described in this paper was designed to document the performance of full-scale field test plots containing GCLs. The test plots were designed to investigate the internal shear strength of these materials, although (as demonstrated by this study) the interface shear strengths were in some cases less than the internal shear strengths and exerted a controlling influence on the behavior of some test plots.

FIELD TEST PLOTS

Fourteen field test plots were constructed at a test site in Cincinnati, Ohio. The layout of the plots is shown in Fig. 1. Five plots (Plots A–E) were constructed on a 3H:1V slope, and nine plots (Plots F–L, N, and P) were built on a 2H:1V slope. Plot P was built where Plot G had originally been located, after a slide occurred at Plot G. An additional plot (M) did not contain a GCL; this plot was constructed to study erosion of surface soils and is not discussed further. Plots on the 2H:1V slope were nominally 20 m long, whereas those on the 3H:1V slope were 29 m long. All plots were two GCL panel widths (~9 m) wide and were covered with 0.9 m of soil.

A typical cross section of a test plot is shown in Fig. 2. In general, the test plots were constructed with a double-sided textured geomembrane overlaying the GCL, which would be typical of a final cover system for a landfill. However, GCLs also are used in final cover systems without geomembranes. Hence, three plots were constructed with no geomembrane. The plots were drained above the geomembrane using a geocomposite drainage layer (geotextile/geonet/geotextile system) or, for the plots that did not contain a geomembrane, a sand drainage layer.

Rationale for 2H:1V and 3H:1V Slopes

The rationale for selecting the 2H:1V and 3H:1V slope inclinations was as follows. The 3H:1V slope was selected to be representative of the typical final cover systems for landfills in use today. To confirm that GCLs are safe against internal failure on 3H:1V slopes, it must be shown that GCLs are not only stable, but are stable with an adequate factor of safety. For an infinite slope consisting of cohesionless interfaces with no seepage, the factor of safety (F) is

$$F = \frac{\tan \phi}{\tan \beta} \tag{1}$$

where ϕ = angle of internal friction; and β = slope angle. Many engineers design permanent slopes to have a minimum factor of safety for static loading of 1.5. The ratio of tan β for a 2H:1V slope to tan β of a 3H:1V slope is 1.5. Subject to the assumptions listed earlier, if a GCL is demonstrated to be stable on a 2H:1V slope (i.e., $F > 1.0$), the same GCL is demonstrated to be stable on a 3H:1V slope with $F > 1.5$. Therefore, the 2H:1V slopes were chosen to demonstrate internal stability of GCLs on 3H:1V slopes with $F > 1.5$. However, it was recognized that constructing 2H:1V slopes was pushing the GCLs to (and possibly beyond) their limits of stability, if not with respect to the internal shear strength of the GCLs, certainly with respect to the various interfaces within the system and perhaps the subsoils, as well.

GCLs Clay Liners

Three types of GCLs, shown schematically in Fig. 3, were used: (1) Geotextile-encased, needle-punched GCLs (Bento-

[1]Prof., and Head of Civ. Engrg., Univ. of Illinois, Urbana, IL 61801.
[2]Dir., Geosynthetic Res. Inst., Drexel Univ., Philadelphia, PA 19104.
[3]Pres., GeoSyntec Consultants, Atlanta, GA 30342.
[4]Consulting Engr., 8580 Kinglet Ln., West Chester, OH 45069.
[5]Proj. Ofcr., U.S. Envir. Protection Agency, Cincinnati, OH 45224.
[6]Geotech. Engr., Haley & Aldrich, Boston, MA 02129.

Note. Discussion open until December 1, 1998. To extend the closing date one month, a written request must be filed with the ASCE Manager of Journals. The manuscript for this paper was submitted for review and possible publication on April 16, 1997. This paper is part of the ***Journal of Geotechnical and Geoenvironmental Engineering***, Vol. 124, No. 7, July, 1998. ©ASCE, ISSN 1090-0241/98/0007-0628–0637/$8.00 + $.50 per page. Paper No. 15587.

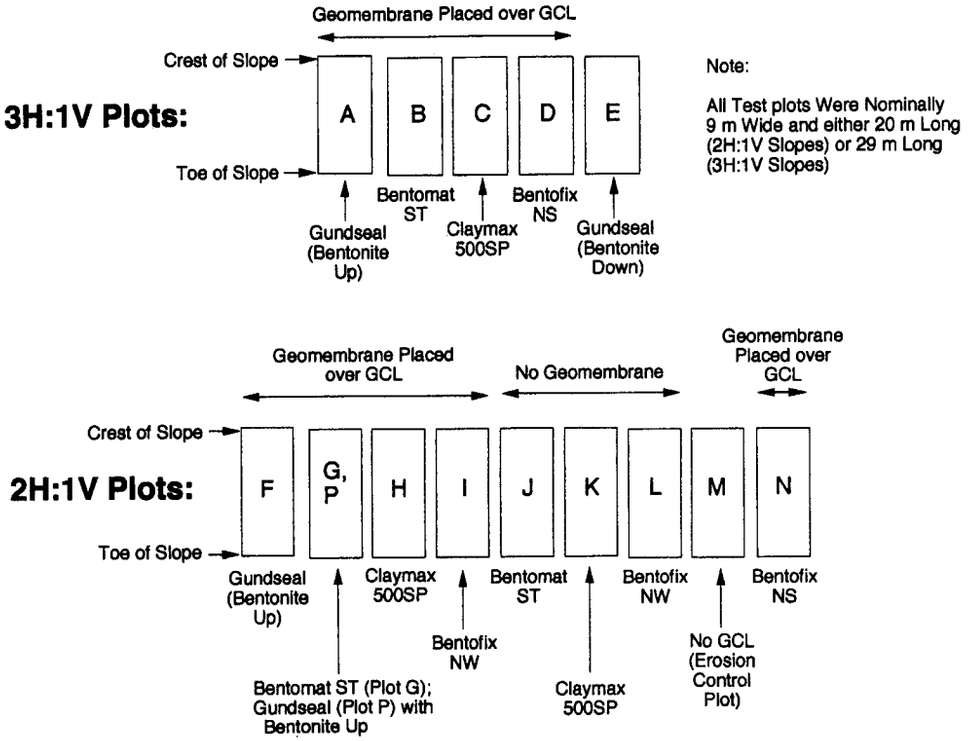

FIG. 1. Layout of Test Plots

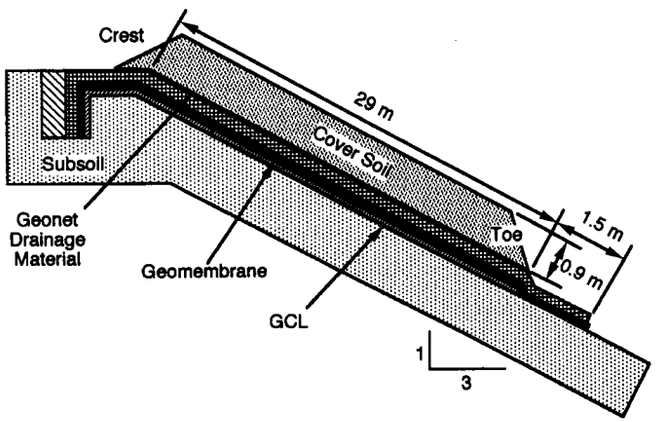

FIG. 2. Cross Section of Test Plots on 3H:1V Slope with Geomembrane Overlying GCL

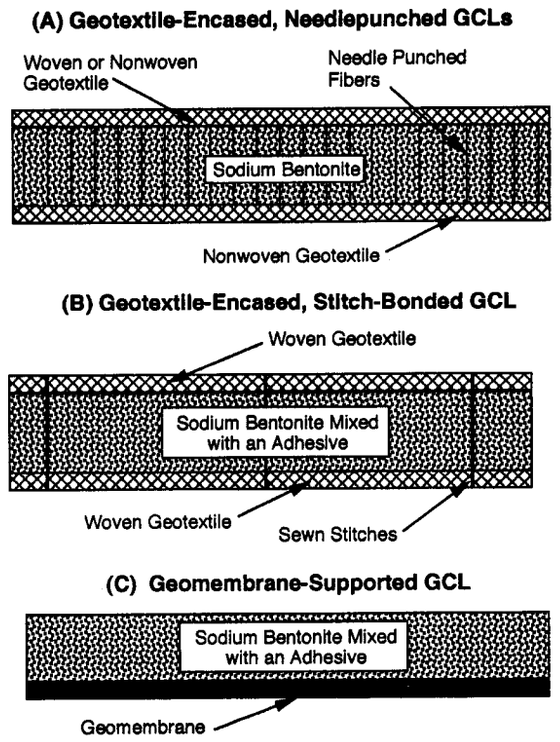

FIG. 3. Types of GCLs Used in Test Plots

mat ST, Bentofix NS, and Bentofix NW); (2) a geotextile-encased, stitch-bonded GCL (Claymax 500SP); and (3) a geomembrane-supported GCL (Gundseal). Table 1 summarizes the type of GCL installed in each plot, the targeted and actual inclinations of the slopes, and the dimensions and cross section of each test plot.

Bentofix NS and Bentomat ST [Fig. 3(a)] consist of bentonite encased between nonwoven and woven geotextiles. Bentofix NW [Fig. 3(a)] consists of bentonite encased between two nonwoven geotextiles. As indicated in Table 1, either the woven or nonwoven geotextile faced upward, depending on the GCL and test plot. Which geotextile component (woven or nonwoven) was in contact with a textured geomembrane turned out to be very important. Fig. 4(a) depicts the cross section for the two test plots (B and G) in which the woven geotextile component of the GCL faced upward and interfaced with a textured high-density polyethylene (HDPE) geomembrane. Fig. 4(b) depicts the cross section for Plots D, I, and N in which the nonwoven geotextile component of the GCLs faced upward and interfaced with an overlying textured HDPE geomembrane. The downward-facing GCL component (interfacing with the subsoil) was a woven geotextile for Plots D and N and a nonwoven geotextile for Plot I.

Claymax 500SP [Fig. 3(b)] consists of bentonite mixed with an adhesive and encased between two woven slit-film geotextiles that are stitched together. Lines of stitching are spaced 100 mm apart. The two geotextile components are identical in this type of GCL.

Gundseal [Fig. 3(c)] is an unreinforced GCL consisting of bentonite mixed with an adhesive and bonded to a geomembrane. The geomembrane component was a textured, 0.8-mm-

TABLE 1. Information on Test Plots

Test plot (1)	Type of GCL (2)	Nominal slope inclination (H:V) (3)	Target slope angle (degrees) (4)	Actual slope angle (degrees) (5)	Actual slope length (m) (6)	Actual plot width (m) (7)	Cross section (top to bottom) (8)	GCL side facing upward (9)	GCL side facing downward (10)
A	Gundseal	3:1	18.4	16.9	28.9	10.5	Soil/GDL/GM/GCL	Bentonite	Geomembrane
B	Bentomat ST	3:1	18.4	17.8	28.9	9.0	Soil/GDL/GM/GCL	Woven GT	Nonwoven GT
C	Claymax 500SP	3:1	18.4	17.6	28.9	8.1	Soil/GDL/GM/GCL	Woven GT	Woven GT
D	Bentofix NS	3:1	18.4	17.5	28.9	9.1	Soil/GDL/GM/GCL	Nonwoven GT	Woven GT
E	Gundseal	3:1	18.4	17.7	28.9	10.5	Soil/GDL/GCL	Geomembrane	Bentonite
F	Gundseal	2:1	26.6	23.6	20.5	10.5	Soil/GDL/GM/GCL	Bentonite	Geomembrane
G	Bentomat ST	2:1	26.6	23.5	20.5	9.0	Soil/GDL/GM/GCL	Woven GT	Nonwoven GT
H	Claymax 500SP	2:1	26.6	24.7	20.5	8.1	Soil/GDL/GM/GCL	Woven GT	Woven GT
I	Bentofix NW	2:1	26.6	24.8	20.5	9.1	Soil/GDL/GM/GCL	Nonwoven GT	Nonwoven GT
J	Bentomat ST	2:1	26.6	24.8	20.5	9.0	Soil/GT/Sand/GCL	Woven GT	Nonwoven GT
K	Claymax 500SP	2:1	26.6	25.5	20.5	8.1	Soil/GT/Sand/GCL	Woven GT	Woven GT
L	Bentofix NW	2:1	26.6	24.9	20.5	9.1	Soil/GT/Sand/GCL	Nonwoven GT	Nonwoven GT
M	Erosion Control	2:1	26.6	23.5	20.5	7.6	Soil	No GCL	No GCL
N	Bentofix NS	2:1	26.6	22.9	20.5	9.1	Soil/GDL/GM/GCL	Nonwoven GT	Woven GT
P	Gundseal	2:1	26.6	24.7	20.5	9.0	Soil/GDL/GM/GCL	Bentonite	Geomembrane

Note: GDL = geocomposite (geotextile/geonet/geotextile) drainage layer; GM = textured geomembrane; GT = geotextile; GCL = geosynthetic clay liner.

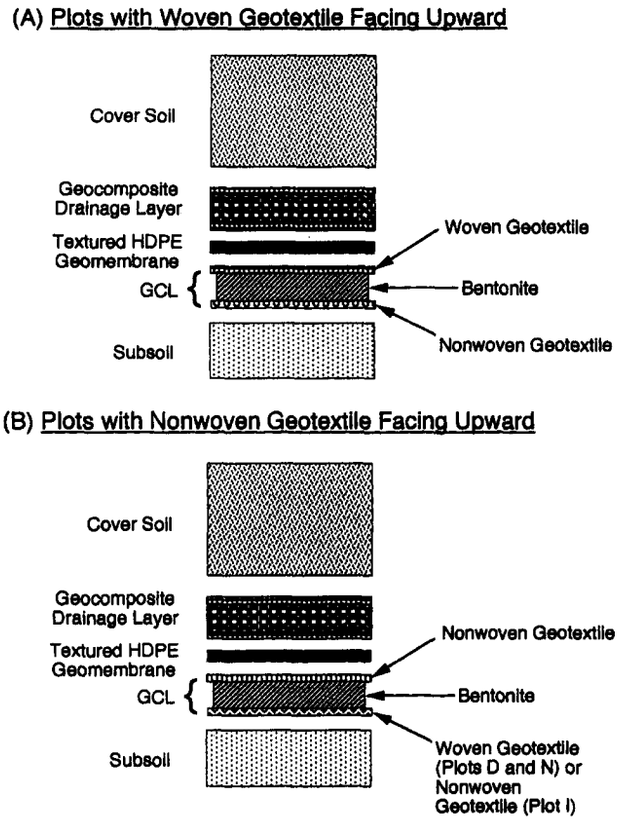

FIG. 4. Cross Sections of Test Plots with Geotextile-Encased GCLs Showing either Woven Geotextile (Plots B and G) or Nonwoven Geotextile (Plots D, I, and N) Interfacing with Textured HDPE Geomembrane

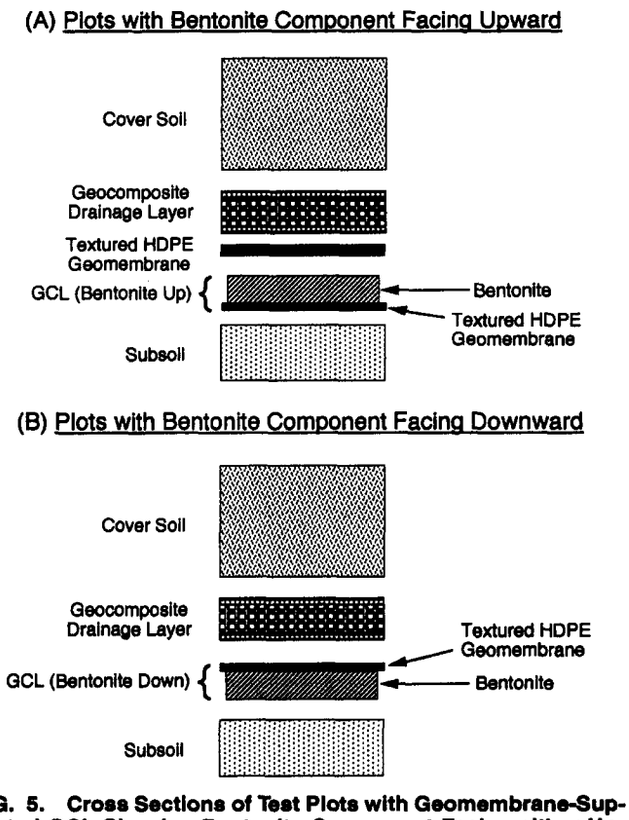

FIG. 5. Cross Sections of Test Plots with Geomembrane-Supported GCL Showing Bentonite Component Facing either Upward (Plots A, F, and P) or Downward (Plot E)

thick HDPE material. With this product, the exposed surface of the bentonite component was covered with a thin geotextile called a "spider net," which is used to help prevent loss or dislodgment of loose particles of bentonite from the GCL during storage, transportation, and installation. The spider net was incorporated in all plots with the geomembrane-supported GCL, except for Plot P, which did not contain the spider net. Fig. 5 shows the two ways in which this type of GCL was used, with the bentonite component either facing upward [Fig. 5(a)] or downward [Fig. 5(b)]. When the bentonite was facing upward (as in Plots A, F, and P), the bentonite was encased between two geomembranes. In this condition, the bentonite was expected to remain essentially dry, except for spot hydration along the overlap or near any imperfections in the overlying geomembrane or geomembrane seams. When the bentonite faced downward (as in Plot E), the bentonite was expected to hydrate by absorbing moisture from the subsoil.

Other Materials

A 1.5 mm (60 mil) textured HDPE geomembrane supplied by National Seal Co. was used for the geomembrane component that was placed on top of the GCL in all test plots except

Plots J, K, and L, which contained no geomembrane. Plot P, which was constructed with the same type and thickness of geomembrane, was supplied by GSE Lining Technologies, Inc. The geocomposite drainage layer consisted of two nonwoven geotextiles heat-bonded to both sides of a geonet. The cover soil was a silty, clayey sand obtained from an on-site borrow source.

Construction

Construction of the test plots began on November 15, 1994 and was completed on November 23, 1994. The only exception is Plot P, which was constructed on June 15, 1995.

The test plots were first graded to provide a smooth subgrade, as shown in Fig. 6. Next, geosynthetics were installed by pulling them down from the crest of the slope (Fig. 7), and then cover soil was placed (Fig. 8) by starting at the bottom of the slope and working upslope. all test plots, except Plot M, were then covered with a geosynthetic erosion control material and seeded with a mixture of grasses.

In plots incorporating a geocomposite drainage layer, the geomembrane and geocomposite were extended beyond the GCL at the toe of the slope and another 1.5 m past the end of the cover soil (Fig. 2). For plots constructed with a sand drainage layer (Plots J, K, and L), a piece of geosynthetic drainage material was embedded in the sand at the toe of the slope and then extended 1.5 m beyond the end of the cover soil.

All of the geosynthetic materials in each test plot were brought into their respective anchor trenches (Fig. 2), which were then backfilled. Because the purpose of each test plot was to test the internal shear strength of a particular GCL, the toe of each test plot was excavated at the completion of construction to the shape shown in Fig. 2 so that no buttressing (i.e., passive) force could be mobilized at the toe of the slope. Similarly, and tension in the geosynthetic components located above the GCL would reduce the shearing stress to be carried by the internal structure of the GCL. To prevent the development of tension in the geosynthetic components above the midplane of the GCL, components above the midplane of the GCL were cut as shown in Fig. 9. Cutting occurred in the spring of 1995, after the winter thaw and about five months after construction of the test plots. However, the geosynthetics were not cut in Plot P, which was constructed later for the purpose of evaluating hydration of bentonite encased between two geomembranes (cutting the geosynthetics would have provided a pathway for water to enter the bentonite near the crest of Plot P).

FIG. 6. Graded Surface of 2H:1V Test Plots Prior to Installation of GCLs

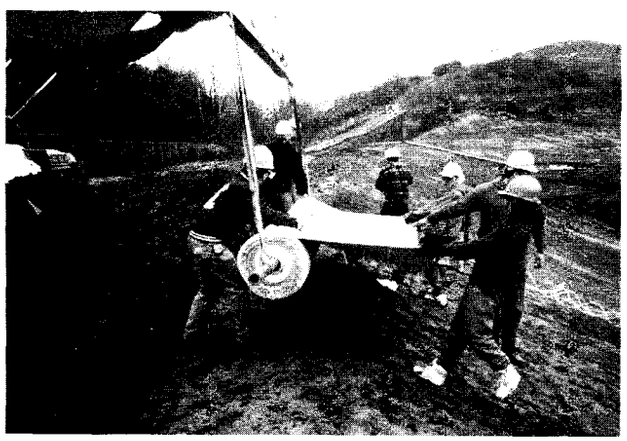

FIG. 7. Installation of GCL on 2H:1V Test Plot

FIG. 8. Placement of Cover Soil from Bottom Upward on 2H:1V Test Plots

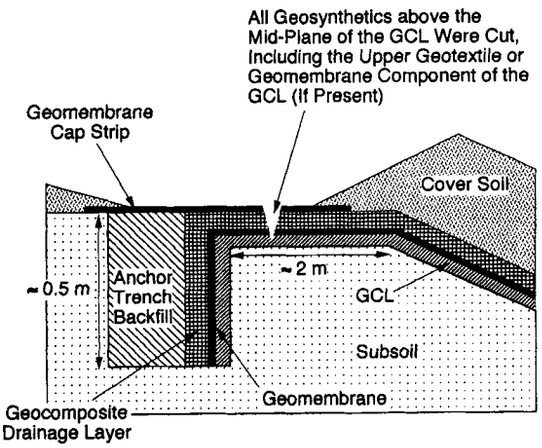

FIG. 9. Cross-Sectional View of Anchor Trench Showing Location where Geosynthetics Were Cut to Transfer Shear Load to the Internal Structure of GCL

INSTRUMENTATION

Instrumentation and calibration of instruments for the field test plots is described by Scranton (1996) and Koerner et al. (1996) and is summarized subsequently.

Moisture Sensors

It was expected that GCLs placed in contact with subgrade soils would hydrate by absorbing moisture from the subgrade. Project-specific testing (Bonaparte et al. 1997) indicated that substantial hydration of GCLs occurred within 10–20 days for GCLs placed in contact with the subgrade soils from the test site, even for subgrade soils compacted at a moisture content

4% dry of the standard Proctor optimum moisture content. Moisture sensors were installed to verify that the bentonite did hydrate. However, in the case of Plots A, F, and P, the bentonite component of the geomembrane-supported GCL was encased between two geomembranes [Fig. 5(a)] with the expectation that the bentonite would remain dry. Thus, for Plots A, F, and P, moisture sensors were installed to verify that the bentonite remained unhydrated.

Gypsum blocks and fiberglass moisture sensors (Daniel et al. 1992) were used to monitor in-situ moisture contents. These instruments were selected based on low cost and the ability to use multiple instruments to provide redundancy. Gypsum blocks were placed in subgrade soils about 50 mm below the GCL. Fiberglass sensors were placed in contact with the GCL, either at the interface between the GCL and subsoil or (for bentonite encased between two geomembranes) between the GCL and geomembrane. Typically, three fiberglass sensors were deployed at each test plot, near the crest, middle, and toe of the slope. However, 16 sensors were installed in Plot P. Moisture sensors were typically monitored every 1–4 weeks.

Displacement Gauges

Displacement gauges (extensiometers) were installed in each test plot (except Plot P, which was constructed only to monitor the moisture content of the bentonite) to measure total and differential displacements in the GCL at multiple locations along the slope. Pairs of stainless steel fish hooks were embedded into both the upper and lower geosynthetic components of a GCL and then glued with epoxy as shown in Fig. 10. A stainless steel wire was attached to the fishhooks and threaded through 6-mm-outside-diameter plastic tubing, which protected the wire and minimized friction between the wire and overlying soil. Each wire extended from the fishhook to a monitoring point about 1.5 m beyond the crest of the slope. During construction, the monitoring point consisted of wooden stakes driven into the soil above the crest of the slope. After construction, the extensiometer wires were connected to a more permanent structure (Fig. 11) at the crest of the slope, where the displacements have been monitored for three years.

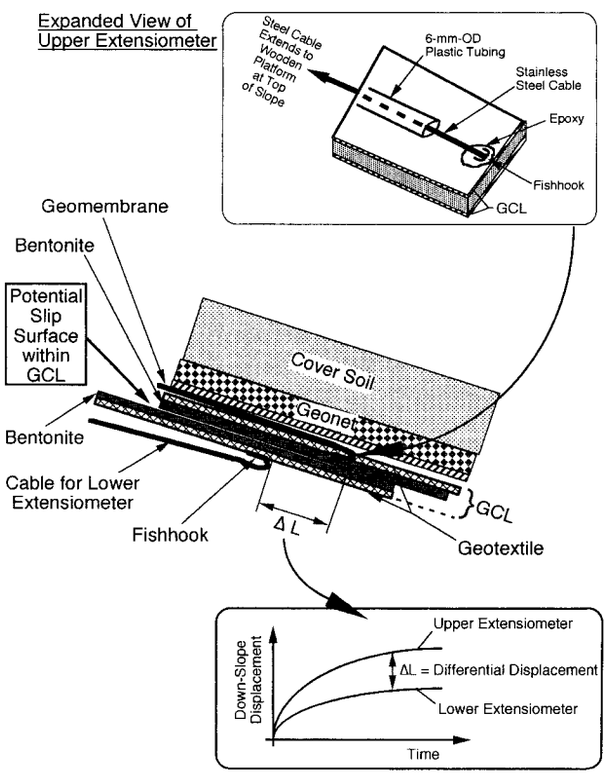

FIG. 10. Displacement Gauges Attached to Upper and Lower Surface of GCL

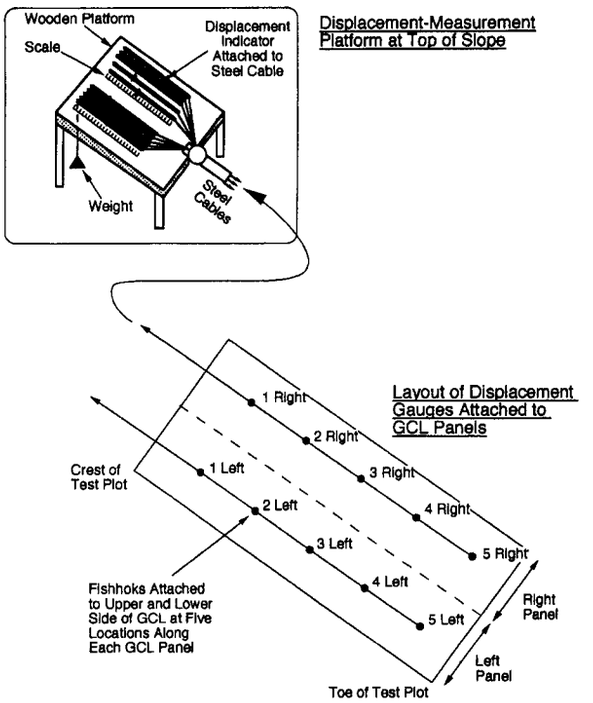

FIG. 11. Locations of Displacement Monitoring Points and Monitoring Table at Top of Slope for Reading Displacement Gauges

Fishhooks were attached to the upper and lower surfaces of each GCL panel at five equally spaced locations along the slope (Fig. 11), resulting in 20 extensiometer monitoring points per test section. The accuracy of the extensiometer measurements was estimated to be $\sim \pm 10$ mm. Displacements were typically measured every 1–4 weeks.

LABORATORY DIRECT SHEAR TESTS

The project schedule did not permit laboratory shear tests to be performed prior to construction. Instead, internal shear strength data from Shan and Daniel (1991), Daniel et al. (1993), and Shan (1993) were used for design of the test plots. Gilbert et al. (1996) and Well (1997) provide additional information on internal shear strength of GCLs. As initial data on the performance of the test plots became available, it became apparent that certain geomembrane-GCL interfaces were more critical with respect to slope stability than the internal shear strength of the GCLs. Thus, the limited laboratory testing program focused on interfaces.

Interfaced direct shear tests were conducted to evaluate textured geomembrane-GCL interfaces and the sand-GCL interface for one GCL. The tests were performed using 300- by 300-mm specimens according to ASTM D5321, with samples taken from the same lots of materials deployed in the field. The GCLs were subjected to a normal load of 17 kPa (equivalent to the field value in the test plots) and then hydrated for 10 days. However, the geomembrane-supported GCL with bentonite encased between two geomembranes was not hydrated because the bentonite in the field was not expected to become hydrated. The rate of shear was 1 mm/min according to ASTM D5321. All tests were single-point tests (i.e., one normal load of 17 kPa). For simplicity of presentation, the test results were interpreted in terms of a secant friction angle (ϕ). Peak and large-displacement (50 mm) secant friction angles are summarized in Table 2.

TABLE 2. Summary of Results of Laboratory Direct Shear Tests

Applicable test plot (1)	Type of GCL (2)	GCL interface component (3)	Opposing interface (4)	Peak secant friction angle (°) (5)	Large-displacement secant friction angle (°) (6)
A,E,F, and P	Gundseal	Dry bentonite	Textured HDPE geomembrane	37	35
B and G	Bentomat ST	Woven slit-film geotextile	Textured HDPE geomembrane	23	21
C and H	Claymax 500SP	Woven slit-film geotextile	Textured HDPE geomembrane	20	20
I	Bentofix NW	Nonwoven needle-punched geotextile	Textured HDPE geomembrane	37	24
K	Claymax 500SP	Woven slit-film geotextile	Drainage sand	31	31
D and N	Bentofix NS	Nonwoven needle-punched geotextile	Textured HDPE geomembrane	29	22

Note: Plots J and L (plots with drainage sand and no geomembrane) were not specifically evaluated because a relatively high-friction angle (31°) was measured for Plot K, which also had drainage sand and no geomembrane.

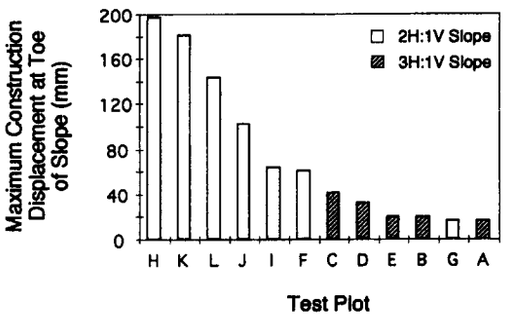

FIG. 12. Summary of Total Downslope Displacement that Occurred during Construction

PERFORMANCE OF TEST PLOTS

Construction Displacements

The displacements that occurred in the GCLs were divided into construction and postconstruction displacements. Displacements were usually largest for the monitoring points located closest to the toes of the slopes (gauges 5-left and 5-right in Fig. 11) and least for monitoring points located closest to the crests of the slopes (gauges 1-left and 1-right in Fig. 11).

Maximum downslope movements measured during construction are summarized in Fig. 12. Total movements were ~20–40 mm for the 3H:1V slopes, and 60–200 mm for the 2H:1V slopes. Differential displacements between the upper and lower surfaces of the GCLs were less than the resolution of the extensiometers (i.e., <10 mm). Mobilization of shear resistance at various interfaces within the system and development of tension in the geosynthetic components caused construction displacements. The test plots with the largest movements during construction for the 2H:1V slopes were Plots H and K and for the 3H:1V slopes was Plot C. All three of these plots contained a geotextile-encased GCL that, with woven slit-film geotextiles on both surfaces, had the lowest interface shear resistance of all of the GCLs tested.

Test Plot G had the lowest displacement of the 2H:1V test plots, probably because the soil at this test plot was less clayey than some of the others and because the component of the GCL in contact with the subsoil was a nonwoven geotextile (nonwoven geotextiles generally have better interface shear resistance with soils than do woven slit-film geotextiles). Plot F had the second lowest movement of the 2H:1V test plots, and plot A had the smallest movement of the 3H:1V plots. In Plots A and F, the textured geomembrane component of the GCL interfaced with the subgrade soil. In general, a textured geo-

TABLE 3. Summary of Performance of Field Test Plots

Plot (1)	Slope (2)	Type of GCL (3)	Stability of test plot as of February 1998 (4)	Maximum total post-construction displacement (mm) (5)	Maximum total post-construction differential displacement (mm) (6)
A	3H:1V	Gundseal	Stable	<10	<10
B	3H:1V	Bentomat ST	Stable	<25	<25
C	3H:1V	Claymax 500SP	Stable	<25	<10
D	3H:1V	Bentofix NS	Stable	<35	<15
E	3H:1V	Gundseal	Stable	<25	<10
F	2H:1V	Gundseal	Slide occurred on March 24, 1996 (internal slide within GCL)	—	750
G	2H:1V	Bentomat ST	Slide occurred on January 12, 1995 (interface slide between lower side of geomebrane and upper woven geotexile component of GCL)	—	25
H	2H:1V	Claymax 500SP	Slide occurred on December 10, 1994 (interface slide between lower side of geomembrane and upper woven geotextile component of GCL)	—	130
I	2H:1V	Bentofix NW	Large deformation in subsoil	<170	<10
J	2H:1V	Bentomat ST	Large deformation in subsoil	<450	<30
K	2H:1V	Claymax 500SP	Large deformation in subsoil	<750	<75
L	2H:1V	Bentofix NW	Large deformation in subsoil	<280	<125
N	2H:1V	Bentofix NS	Stable	<30	<10
P	2H:1V	Gundseal	Stable	NA	NA

Note: Total deformation is the total amount of downslope movement; differential deformation is the difference between downslope movement of the upper and lower surfaces of the GCL.

TABLE 4. Summary of Calculated Factor of Safety (F) and Actual Slope Stability

Test plot (1)	Slope angle (°) (2)	Peak friction angle (°) (3)	Large-displacement friction angle (°) (4)	Peak F (5)	Large displacement F (6)	GCL performance (7)
A	16.9	37 (D)[a]	35 (D)[a]	2.5 (D)[a]	2.3 (D)[a]	Stable
B	17.8	23[b]	21[b]	1.3[b]	1.2[b]	Stable
C	17.6	20[b]	20[b]	1.1[b]	1.1[b]	Stable
D	17.5	29[b]	22[b]	1.8[b]	1.3[b]	Stable
E	17.7	20 (H)[a]	20 (H)[a]	1.1 (H)[a]	1.1 (H)[a]	Stable
F	23.6	20 (H)[a]	20 (H)[a]	0.8 (H)[a]	0.8 (H)[a]	Internal Slide
G	23.5	23[b]	21[b]	1.0[b]	0.9[b]	Internal Slide
H	24.7	20[b]	20[b]	0.8[b]	0.8[b]	Internal Slide
I	24.8	37[b]	24[b]	1.6[b]	1.0[b]	Stable[d]
J	24.8	~31[b]	~31[b]	1.3[b]	1.3[b]	Stable[d]
K	25.5	31[b]	31[b]	1.3[b]	1.3[b]	Stable[d]
L	24.9	~31[b]	~31[b]	1.3[b]	1.3[b]	Stable[d]
N	22.9	~37[b]	~24[b]	1.8[b]	1.1[b]	Stable

[a]Internal GCL strength for dry (D) or hydrated (H) bentonite.
[b]GCL-geomembrane interface.
[c]GCL-drainage sand interface.
[d]Large displacement occurred in subsoil below GCL, but not in or at the interface with GCL.

membrane also has comparatively good interface shear resistance (generally better than a woven slit-film geotextile).

Postconstruction Performance of 3H:1V slopes

Postconstruction displacements are summarized in Table 3. All 3H:1V slopes have remained stable during the three years of observation. Total downslope displacements have been <35 mm, and differential displacements have been <10–25 mm. No visual evidence of displacement or surface cracking exists.

Test Plot A (Bentonite between Two Geomembranes)

The bentonite component of the GCL was expected to remain dry because the bentonite was encased between two geomembranes. As indicated in Table 4, measured peak and large-displacement interface secant friction angles between dry bentonite and textured HDPE were 37 and 35°, respectively. Since the slope angle was 16.9°, the slope should be stable as long as the bentonite remains dry. Calculated factors of safety [(1)] for interface failure, summarized in Table 4, range from 2.3 to 2.5 for Plot A.

Fiberglass moisture sensors in Plot A have provided variable results; two of the three moisture sensors have indicated that the bentonite has remained dry, but one sensor near the crest of the slope has indicated some hydration. Two borings were drilled by hand near the crest and toe of the test plot in March 1995, and 100-mm-diameter samples of the GCL were removed. The water contents of the bentonite in the GCL at the crest and toe were 27 and 24%, respectively. These values are essentially identical to the water content at the time of installation, confirming that the bentonite had not hydrated. Individual fiberglass moisture sensors have been found during calibration to have relatively large scatter (Scranton 1996). However, the trends indicated by the majority of the moisture sensors at any one test plot have been verified when direct sampling and moisture content determination were performed.

Test Plots B, C, and D (Geotextile-Encased GCLs)

The bentonite in these geotextile-encased GCLs was expected to hydrate by absorbing moisture from subgrade soils. Most of the fiberglass moisture sensors have indicated that the bentonite has hydrated, although less than expected. One factor inhibiting hydration may have been the relatively dry, sandy subsoils on the 3H:1V test plots, compared to the 2H:1V test plots, which had more clayey, wetter subsoils.

Experience has shown that GCL interface shear strengths are typically less than internal shear strengths for internally reinforced GCLs such as those used in Test Plots B, C, and D, when tested at low normal stress (Gilbert et al. 1996). Peak interface secant friction angles between the upward-facing geotextile component of the GCLs and the textured HDPE geomembrane were found to be 20–29°, and large-displacement friction angles were found to be 20–22° for essentially full hydration of the GCL. The test plots have remained stable because the slope angles are 17.5–17.8°, i.e., less than the interfacial friction angles. The calculated factors of safety for an interface failure for Plots B–D range from 1.1 to 1.8 (Table 4).

Test Plot E (Unreinforced GCL)

Test Plot E was constructed with the bentonite portion of the geomembrane-supported GCL facing downward. Interface shear tests were not performed on the hydrated GCL because the internal shear strength under consolidated-drained conditions had already been studied. These previous tests were performed on fully hydrated samples at water contents of approximately 150%. Resulting interface shear strengths were found to vary with normal stress (Fig. 13). For the normal stress acting on the GCL in Test Plot E (17 kPa), the drained angle of internal friction for fully hydrated bentonite is approximately 20°. The slope angle at Plot E was 17.7°. Thus, Plot E is expected to be stable, but only with $F = \tan(20°)/\tan(17.7°) = 1.1$ for an infinite slope.

As with most of the other test plots, the fiberglass moisture sensors for Plot E have yielded variable results, with some sensors indicating that the bentonite has become hydrated and others indicating that it has not become hydrated. A boring was drilled and a sample was taken from near the crest of the slope (the driest area) in March 1995, and the water content

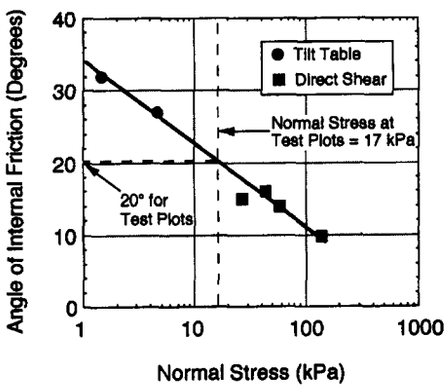

FIG. 13. Variation of Secant Angle of Internal Friction with Normal Stress for Hydrated Bentonite in Gundseal Sheared under Consolidated-Drained Conditions [from Shan (1993)]

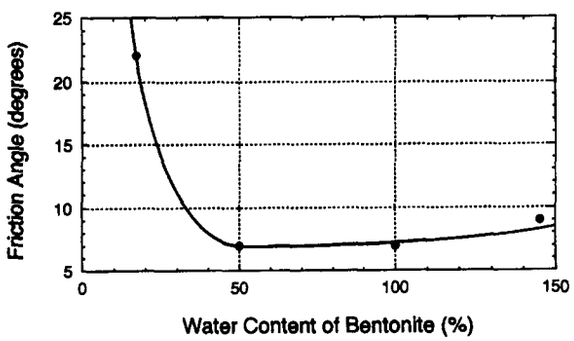

FIG. 14. Influence of Water Content of Bentonite on Drained Angle of Internal Friction [from Daniel et al. (1993)]

of the bentonite was found to be 46%. Eight more borings were drilled in April 1996, at various locations along the full length of the slope. The water content varied between 54 and 79%, and averaged 60%. Daniel et al. (1993) previously measured the shear strength of the bentonite component of this same type of geomembrane-supported GCL as a function of water content using a direct shear apparatus and a slow rate of shear that allowed excess pore water pressures to dissipate fully. The range of normal stress used in the testing program was 27–139 kPa. The highest water content (~145%) was achieved by fully hydrating the bentonite. Results, plotted in Fig. 14, show that once the water content of the bentonite reaches 50% or more, the shear strength declines to a value approximately equal to the strength of fully hydrated bentonite. In other words, the bentonite does not have to be fully hydrated for bentonite's strength to be greatly reduced. This fact is obvious from handling a GCL; at 50% water content, the bentonite feels hydrated and very slick. Thus, the average water content of 60% in Test Plot E should be sufficiently large to replicate the strength reduction associated with full hydration of the bentonite.

Postconstruction Performance of 2H:1V Plots

Most of the GCLs at the 2H:1V test plots have remained stable (though there has been displacement in the subsoils at many plots), but there have been slides involving GCLs at Plots F, G, and H. All three slides occurred as massive block slides. Two of the slides are shown in Fig. 15. The surfaces of the two plots appear different because different erosion control materials were placed on the surfaces. The white materials on the upper portions of the slopes are the GCLs, which remained intact. Before these two slides are analyzed, however, Plots F and P are discussed.

Test Plots F and P (Bentonite between Two Geomembranes)

Plots F and P, like Plot A, contained bentonite encased between two geomembranes. The bentonite in these test plots was expected to remain dry. However, within three months after Plot F was constructed, two of the three moisture sensors indicated that the bentonite had become hydrated.

To evaluate the condition of the bentonite, 17 borings were drilled into Plot F in March 1995, and 100-mm-diameter samples of the GCL were recovered. The water content of the bentonite samples varied from 10 to 188%, and the data showed that the right panel was much more hydrated than the left panel. In contrast to these field data, Estornell and Daniel (1992) reported laboratory test results for this same GCL in which water migrated laterally through the geomembrane-encased bentonite less than 100 mm over a test duration of six months.

FIG. 15. Photograph of Slides Involving Plot G (Left) and Plot H (Right)

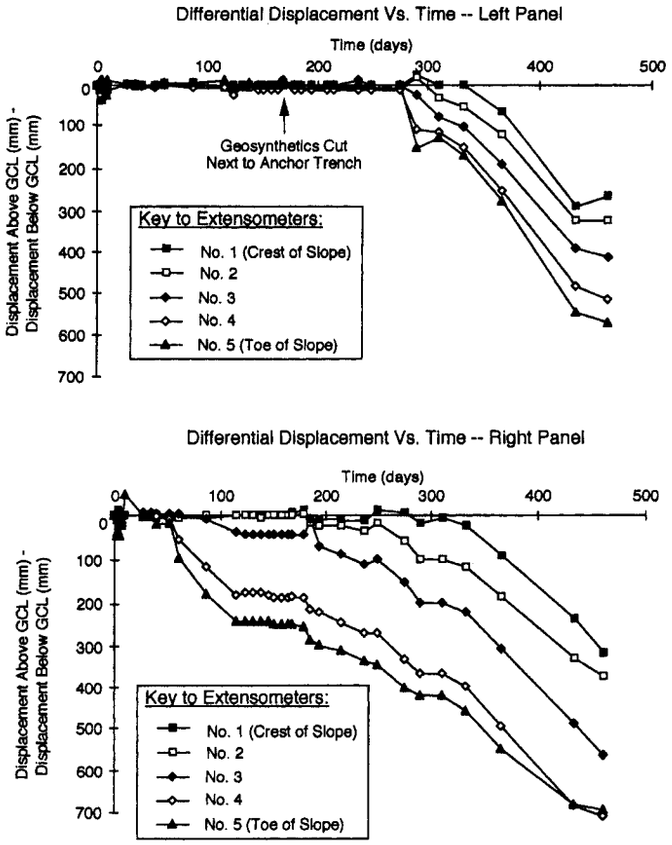

FIG. 16. Deformations in Plot F

Plot F was located at a point where surface water at the crest of the slope was funneled directly to the anchor trench area where penetrations were made for the extensiometer cables. Water may have entered the bentonite through cuts made in the geomembrane for the extensiometer cables or from the edges of the plots where drainage trenches were located. Once water entered the bentonite, the mechanism for lateral movement was probably through small gaps beneath occasional wrinkles or waves in the overlying geomembrane that were not completely smoothed out during installation. Unfortunately, the plot slid before a complete forensic study could be performed.

Displacement sensors showed large movements in the right panel of Plot F during the first period of observation, but not in the left panel (Fig. 16). About 275 days after starting construction (August 1995), the left panel began to move downslope, suggesting that the bentonite in the left panel also was starting to become hydrated.

Plot F slid on March 24, 1996, 495 days after construction began. The cause of the slide is hydration of the bentonite; the peak angle of internal friction for hydrated bentonite at the normal stress existing in the field was 20°, but the slope angle was 23.6° (factor of safety, $F = 0.8$, for internal failure). In contrast, the peak interface friction angle for dry bentonite was 37°. Had the bentonite not hydrated, the slope should have remained stable.

In response to the unexpected hydration, Plot P was constructed at the location of the former Plot G on June 15, 1995. Extensiometers were not installed in Plot P to eliminate all penetrations in the overlying geomembrane. The number of fiberglass moisture sensors in the bentonite was increased from 3 in the other test plots to 16 in Plot P to provide additional documentation of moisture conditions. All but 1 of the 16

moisture sensors have indicated that the bentonite has remained dry after more than two years of monitoring Plot P. Plot P would not have remained stable had the bentonite become hydrated.

It appears that of the three plots for which bentonite was encased between two geomembranes (Plots A, F, and P), the bentonite has remained dry at two plots (Plots A and P), and has become hydrated at one (Plot F). The lesson learned seems to be that geomembranes above and below the bentonite block access to water, but if water can contact the bentonite, it can spread along wrinkles or waves in the geomembrane. The keys to keeping bentonite dry appear to be limiting access of the bentonite to water and limiting the ability of water to spread by minimizing waves or wrinkles in the geomembrane.

Test Plots G and H

Test Plots G and H consisted of geotextile-encased GCLs. Both plots slid (Fig. 15) at the interface between the upper geotextile (a woven slit-film geotextile in both cases) and the lower surface of the overlying textured HDPE geomembrane. Plot H slid 20 days after construction, ad Plot G slid 50 days after construction. Preslide displacements were small (<25–130 mm). There was no warning of either slide. Both slides occurred when no one was observing the plots, and the slides apparently occurred quickly.

Test Plot H was constructed on a 24.7° slope, but the measured peak and large-displacement interface friction angles for the relevant materials under hydrated conditions were only 20°, yielding a factor of safety of 0.8 (Table 4) for interface failure. Test Plot H did not slide immediately because the interfacial shear strength of the dry GCL was sufficient to maintain a stable slope. The slope slid when the bentonite hydrated sufficiently to drop the factor of safety below 1.0. Tests reported by Bonaparte et al. (1997) showed that bentonite in the GCLs hydrated in a period of 10–20 days when placed in contact with the subgrade soils from the test plots. Tests reported by Daniel et al. (1993) indicated similar periods of hydration of the bentonite in GCLs for other soils. Thus, the sliding time of 20 days after construction is consistent with the expected time required for the bentonite to absorb moisture from subgrade soils.

When GCLs containing a woven geotextile component become hydrated, bentonite can extrude through the openings of the geotextile and lubricate the GCL-geomembrane interface (Gilbert et al. 1996). After the slide, the surface of the GCL was very slick. The tendency of bentonite to lubricate the geomembrane-GCL interface is related to the openings between yarns in the woven slit-film geotextile. The size of these openings is essentially impossible to control because there is no bonding at the points of yarn contact.

Test Plot G was slower to slide, but the slope angle (23.5°) was 1.2° flatter than for Plot H, and the interface shear strength between the GCL and overlying geomembrane (23° peak, 21° large displacement) was 1–3° higher. Also, a nonwoven geotextile faced downward in Plot G, but a woven slit-film geotextile faced downward in Plot H. GCLs absorb water more slowly from subgrade soils when the geotextile separating the bentonite from the subsoil is a thicker nonwoven geotextile (Jahangir 1994). Thus, the reason why Plot G slid 30 days later than Plot H is that the bentonite in the GCL at Plot G was separated from wet subgrade soils by a thicker, nonwoven geotextile, which slowed hydration. The calculated factor of safety for Plot G ranged from 0.9 to 1.0 for interface failure under hydrated conditions (Table 4).

Plots I and N with Nonwoven Geotextile Component Facing Upward

Plots I and N are similar to Plot G, except that the GCL contained either one nonwoven geotextile with the nonwoven geotextile facing upward (Plot N) or two nonwoven geotextiles (Plot I). The slope angles at Plots I and N were similar to the other 2H:1V plots. However, the interface friction angle between the nonwoven geotextile component of the GCL and the textured HDPE (37° peak and 24° large displacement) was much greater than for the woven slit-film geotextile component of the GCLs that slid. The GCLs and their interfaces have remained stable at Plots I and N because of the higher interface shear resistance between a nonwoven geotextile component of a GCL compared to a woven geotextile component. The higher interface shear resistance from the nonwoven geotextile is attributed to (1) larger shear resistance developed between nonwoven geotextiles and textured geomembranes in general; and (2) less hydrated bentonite extrusion to the interface for the thicker nonwoven geotextile. The calculated factors of safety for Plots I and N range from 1.1 to 1.8 (Table 4) for interface failure.

FIG. 17. Photograph of Scarp at Plot I Created by Slide in Subsoil beneath Test Plot

After 2 1/2 years of monitoring, the total downslope movement of Plot I had reached ~170 mm near the toe of the slope, when a slide occurred in the subsoil beneath the GCL (Fig. 17). Excavation into the scarp revealed that the sliding surface was located about 1 m below the GCL and within a wet, plastic clay material. In this case, the GCLs and their interfaces were actually stronger than the native subsoils. Similar failures in foundation soils occurred in nearby plots.

Plots J, K, and L with No Geomembrane

These plots were constructed by placing drainage sand directly above the GCL. The GCLs at all three test plots have remained stable, although total displacements, which were negligible during the first year of observation, increased to 280–750 mm (Table 3) by the end of the third year of observation. The peak secant interface friction angle between the sand drainage material and GCL was 31° for a woven slit-film component (Table 2) and, although not measured, presumably more for a nonwoven component. An interface friction angle of 31° is significantly greater than the slope angle (~25°), resulting in a computed factor of safety of 1.3 for interface failure, which explains the stability of the GCLs and their interfaces in these test plots.

Large displacements have occurred in the foundation soils at Plots I, J, and K, similar to the displacements at Plot I (Fig. 17). The displacements developed in the subsoils beneath the test plots during the wet spring season of 1997. Sliding occurred in some plots, but as shown in Fig. 17, the sliding occurred below the GCLs. Again, the GCLs and their interfaces were stronger than the foundation soils.

CONCLUSIONS

Fourteen test plots, designed to replicate typical final cover systems for solid waste landfills, were constructed to evaluate the internal shear strength of GCLs under full-scale field conditions on 2H:1V and 3H:1V slopes. Five different types of GCLs were evaluated. The test plots have been observed for over three years. All test plots were initially stable, but over time as the bentonite in the GCLs became hydrated, three slides (all on 2H:1V slopes) involving GCLs have occurred. One slide involved an unreinforced GCL in which bentonite that was encased between two geomembranes unexpectedly became hydrated. The other two slides occurred on 2H:1V slopes at the interface between the woven geotextile components of the GCLs and the overlying textured HDPE geomembranes.

The experience from these test plots provides several conclusions of practical significance to engineers. At the low normal stresses associated with landfill cover systems, the interface shear strength is generally lower than the internal shear strength of internally reinforced GCLs. The key (weakest) interface, should it exist, will typically be between a woven geotextile component of the GCL and the adjacent material, which in this case was a textured HDPE geomembrane. The interface strength may be low in part because of the tendency of bentonite to extrude through the openings in the relatively thin, woven geotextile and then into the interface as the GCL hydrates. Design engineers are encouraged to consider GCLs with relatively thick, nonwoven geotextile components in critical situations where high interface shear strength is required.

Current engineering practice for evaluating the stability of GCLs on slopes is to conduct direct shear tests and then to use limit-equilibrium methods of slope stability analysis to calculate factors of safety based on the results of those tests. The experience from the test plots has validated this process. All three test plots that slid had calculated factors of safety of less than 1.0. All remaining (stable) test plots had factors of safety greater than 1.0. Although technical issues associated with internal and interface direct shear testing of GCLs remain, it is gratifying to have documented field data that substantiate the current design process.

Engineers can design stable slopes with GCLs and take advantage of the excellent hydraulic properties of these materials, but engineers must not design slopes that exceed the safe slope angle for the GCLs or their respective interfaces within the system. Based on the experience from this study, 2H:1V slopes are too steep to be stable with a factor of safety normally considered adequate, but 3H:1V slopes (depending on materials) can be constructed with factors of safety of at least 1.5 for the conditions existing in this project, and probably many others, as well.

The writers plan to continue monitoring of the remaining test plots for several more years.

ACKNOWLEDGMENTS

The research described in this paper has been funded primarily by the U.S. Environmental Protection Agency (EPA) under cooperative agreement CR-821448. The EPA's Project Officers on this project were Robert E. Landreth (retired) and David A. Carson. This paper has not been subjected to the agency's peer and administrative review. The findings do not necessarily reflect the views of the agency. Mention of trade names or commercial products does not constitute endorsement or recommendation for use. Additional financial support was provided by Claymax Corp. (now CETCO), Gundle (now GSE) Lining Systems, and National Seal Co. Akzo, Synthetic Industries, and Tensar provided erosion control materials, James Anderson, John Bowders, Richard Carriker, Mark Cadwallader, Ted Dzierzbicki, Richard Erickson, John Fuller, George Koerner, Larry Lydick, Majdi Othman, Fred Struve, and Robert Trauger made major contributions to the program, which are gratefully acknowledged. Finally, the writers thank Waste Management of North America and the staff of the Elda Landfill in Cincinnati, Ohio (especially John Stark and David Bower) for providing space at the landfill for the test plots and for providing personnel and equipment to assist with construction and maintenance.

APPENDIX. REFERENCES

Bonaparte, R., Othman, M. A., Rad, N. S., Swan, R. H., and Vander Linde, D. L. (1997). "Evaluation of various aspects of GCL performance." *1995 Workshop on Geosynthetic Clay Liners, Rep. No. EPA/600/R-96/149*, U.S. Envir. Protection Agency, Washington, D.C., F1–F34.

Daniel, D. E., Burton, P. M., and Hwang, S. D. (1992). "Evaluation of four vadose zone probes used for leak detection and monitoring." *Current practices in ground water and vadose zone investigations, ASTM STP 1118*, D. M. Nielsen and M. N. Sara (eds.), American Soc. for Testing and Mat., Philadelphia, Pa., 124–139.

Daniel, D. E., and Koerner, R. M. (1995). *Waste containment systems: Construction, quality assurance, and quality control*. ASCE, Reston, Va., 354.

Daniel, D. E., Shan, H. Y., and Anderson, J. D. (1993). "Effects of partial wetting on the performance of the bentonite component of a geosynthetic clay liner." *Proc., Geosynthetics '93*, Industrial Fabrics Assn. Int., St. Paul, Minn., 3, 1483–1496.

Estornell, P., and Daniel, D. E. (1992). "Hydraulic conductivity of three geosynthetic clay liners." *J. Geotech. Engrg.*, ASCE, 118(10), 1592–1606.

Gilbert, R. B., Fernandez, F., and Horsfield, D. W. (1996). "Shear strength of reinforced geosynthetic clay liner." *J. Geotech. Engrg.*, ASCE, 122(4), 259–266.

Jahangir, M. A. (1994). "Containment of petroleum hydrocarbons by geosynthetic clay liners using natural soil moisture," MS thesis, Univ. of Texas at Austin, Austin, Tex., 200.

Koerner, R. M. (1994). *Designing with geosynthetics*, 3rd Ed., Prentice-Hall, Englewood Cliffs, N.J., 783.

Koerner, G. R., Bowders, J. J., and Scranton, H. B. (1996). "Instrumentation for monitoring field performance of the cincinnati GCL test plots." *Proc., GRI-10 on Field Performance of Geosynthetics and Geosynthetic Related Sys.*, Geosynthetics Information Inst., Drexel Univ., Philadelphia, Pa., 176–201.

Koerner, R. M., and Gartung, E. (1995). *Geosynthetic clay liners*. A. A. Balkema, Rotterdam, The Netherlands, 245.

Mesri, G., and Olson, R. E. (1970). "Shear strength of montmorillonite," *Geotechnique*, London, England, 20(3), 261–270.

Olson, R. E. (1974). "Shearing strengths of kaolinite, illite, and montmorillonite." *J. Geotech. Engrg. Div.*, ASCE, 100(11), 1215–1229.

Scranton, H. B. (1996). "Field performance of sloping test plots containing geosynthetic clay liners," MS thesis, Univ. of Texas at Austin, Austin, Tex., 206.

Shan, H. Y. (1993). "Stability of final covers placed on slopes containing geosynthetic clay liners," PhD dissertation, Univ. of Texas at Austin, Austin, Tex., 296.

Shan, H. Y., and Daniel, D. E. (1991). "Results of laboratory tests on a geotextile/bentonite liner material." *Proc., Geosynthetics '91*, Industrial Fabrics Assn. Int., St. Paul, Minn., 2, 517–535.

Well, L. W. (1997). *Testing and acceptance criteria for geosynthetic clay liners, ASTM STP 1308*. American Soc. for Testing and Mat., Philadelphia, Pa., 268.